

Carbon sequestration monitoring with acoustic double-difference waveform inversion: A case study on SACROC walkaway VSP data

Di Yang*, Michael Fehler, and Alison Malcolm, MIT; Lianjie Huang, Los Alamos National Laboratory

SUMMARY

Geological carbon sequestration involves large-scale injection of carbon dioxide into underground geologic formations and is considered as a potential approach for mitigating global warming. Changes in reservoir properties resulting from the CO₂ injection and migration can be characterized using waveform inversions of time-lapse seismic data. The conventional approach for analysis using waveform tomography is to take the difference of the images obtained using baseline and subsequent time-lapse datasets that are inverted independently. By contrast, double-difference waveform inversion uses time-lapse seismic datasets to jointly invert for reservoir changes. We apply conventional and double difference methods to a field time-lapse walkaway VSP data set acquired in 2008 and 2009 for monitoring CO₂ injection at an enhanced oil recovery field at SACROC, Texas. The double-difference waveform inversion gives a cleaner and more easily interpreted image of reservoir changes, as compared to that obtained with the conventional scheme. Our results from the application of acoustic double-difference waveform tomography shows some zones with decreased P-wave velocity within the reservoir due to CO₂ injection and migration.

INTRODUCTION

Time-lapse seismic monitoring is widely used in reservoir management in the oil industry to obtain information about reservoir changes caused by fluid injection and subsequent production of fluids from heterogeneous reservoirs. Changes in reservoirs during large-scale CO₂ injections, for reducing CO₂ emissions, are also observed using time-lapse seismic surveys. The long-term monitoring of underground CO₂ injection zones to characterize fluid migration and potential leakage over time is crucial for ensuring safe and reliable carbon storage (Bickle et al., 2007).

Conventional analysis of time-lapse seismic data only gives qualitative information (Arts et al., 2004). Impedance contrasts and seismic response changes have been used to characterize CO₂ accumulations in thin layers, and "velocity push-down effects" that cause slower propagation of seismic waves through the CO₂ saturated area have been identified. However, these changes have not been quantified. Waveform inversion has the potential to estimate subsurface density and elasticity parameters quantitatively (Tarantola, 1984), and it is becoming more feasible with the increasing computing power. Ideally, by subtracting the images inverted from each data set in a series of time-lapse surveys, the geophysical property changes over time can be quantified. However, independent waveform inversions are affected by data quality, survey design, and computational parameters used in the inversion, which can be different between surveys, and lead to noisy images. For these rea-

sons, a direct subtraction of images can produce spurious results. Watanabe et al. (2005) applied a differential waveform tomography in the frequency domain for crosswell time-lapse data during gas production, and showed that the results are more accurate for estimating velocity changes in small regions than those obtained using the conventional method. Onishi et al. (2009) also applied a similar strategy to conduct differential traveltimes tomography using crosswell surveys. Denli and Huang (2009) developed a double-difference waveform tomography algorithm using time-lapse reflection data in the time domain and demonstrated using synthetic data that the method has the potential to produce reliable estimates of reservoir changes.

In this work, we apply the acoustic double-difference methodology to the time-lapse walkaway VSP data acquired in 2008 and 2009 for monitoring CO₂ injection at an enhanced oil recovery (EOR) field at SACROC, Texas. The baseline data were acquired in 2008 before CO₂ injection. The objective of the SACROC project is to investigate the combination of carbon sequestration and enhanced oil recovery. Our double-difference waveform inversion reveals a zone with decreased velocity within the reservoir. This could be due to the CO₂ injection. We compare our results with that obtained by subtracting two images obtained using independent waveform inversions, and show that double-difference waveform inversion produces a cleaner and more informative image of the reservoir change than the conventional approach.

THEORY

The procedure for double-difference waveform inversion consists of two parts. The first one is a traditional waveform inversion of the baseline survey data using an initial model obtained from a preliminary velocity analysis. Waveform inversion minimizes a cost/objective function of the difference between modeling data and baseline data:

$$E(m) = \frac{1}{2} \|u_{baseline} - u_{modeling}\|^2 = \frac{1}{2} \delta u^T \delta u \quad (1)$$

where $u_{baseline}$ and $u_{modeling}$ are the displacements of baseline data and forward modeling, respectively, $\delta u = u_{modeling} - u_{baseline}$, the superscript T denotes the transpose, and m is the parameter (P-wave velocity) to be updated.

The gradient of the objective function is derived by taking its derivative with respect to m , leading to

$$\nabla_m E = \frac{\partial E(m)}{\partial m} = \left(\frac{\partial u_{modeling}}{\partial m} \right)^T \delta u \quad (2)$$

The gradient can be calculated efficiently by cross-correlating the forward propagating wavefields from sources with the back propagating residual wavefield from receivers (Tarantola, 1984). Based on the assumption that the initial model is close to the

Double-difference waveform inversion

true solution, the objective function can be minimized via the Gauss-Newton or steepest descent methods. Due to the computational cost of calculating the Hessian matrix (Sheen et al., 2006), we use the nonlinear conjugate gradient method that does not require the Hessian matrix, and has a better convergence rate than the steepest descent method (Rodi and Mackie, 2001).

The model parameter is updated in each iteration according to

$$m_{i+1} = m_i - \alpha \vec{G}_{i+1} \quad (3)$$

where \vec{G}_{i+1} is the search direction defined by the gradient of the current step $\nabla_m E_{i+1}$ and the search direction of the previous step \vec{G}_i (Rodi and Mackie, 2001). The parameter α is the step length obtained from a line search algorithm to reach the minimum cost in each iteration.

After the inversion of the baseline data, the model that best approximates most of the wave events in the baseline data is used as the initial model in the double difference waveform inversion for time-lapse data. The double-difference inversion is very similar to the inversion scheme described above, with a modification to the cost function to be

$$\delta u = (u_{\text{lapse}} - u_{\text{baseline}}) - (u_{\text{modeling}} - u_{\text{baselinemodel}}) \quad (4)$$

where u_{baseline} and u_{lapse} are baseline and time-lapse data, and $u_{\text{baselinemodel}}$ and u_{modeling} are synthetics from the starting model obtained from inversion of the baseline data and the model to be updated, respectively. Double-difference waveform inversion inverts for the change in the model that causes the waveform changes between time-lapse datasets. It can reduce the effects of both noise and uncertainties in the initial model.

TIME-LAPSE WALKAWAY VSP DATA FROM SACROC

We apply the acoustic double-difference waveform tomography method to time-lapse walkaway VSP data collected at the Scurry Area Canyon Reef Operators Committee (SACROC) field in West Texas for monitoring CO₂ injection. The schematic configuration of the surveys is shown in Figure 1. Two walkaway VSP datasets were acquired in the same well in July 2008 and April 2009. The baseline data were acquired before CO₂ injection. The walkaway line is oriented north-south. Vibrators were used as sources, and were spaced at intervals of 36.56 meters, with a total of 100 shot points acquired. The best-quality data from 97 shot points were used in inversion. The data were collected in the monitoring well using 13 receivers at depths ranging between 1554.5 to 1737.4 meters and spaced at an interval of 15.24 meters. Between the two surveys, CO₂ was injected through injection wells close to the monitoring well. The reservoir is located between depths of about 1820 to 2100 meters.

DATA PROCESSING

The downgoing wavefields and upgoing wavefields of the VSP data were separated using the method of (Cheng et al., 2010),

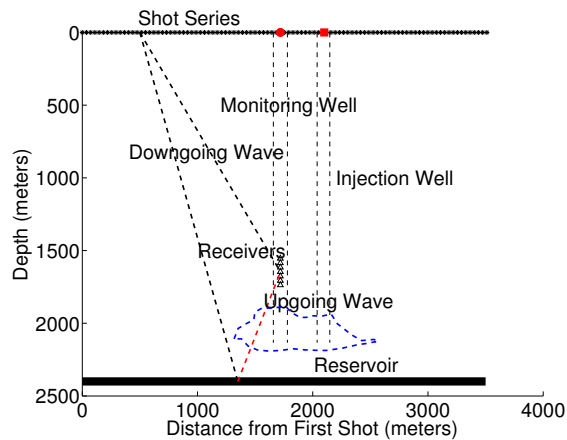


Figure 1: The schematic configuration of the walkaway VSP surveys at SACROC.

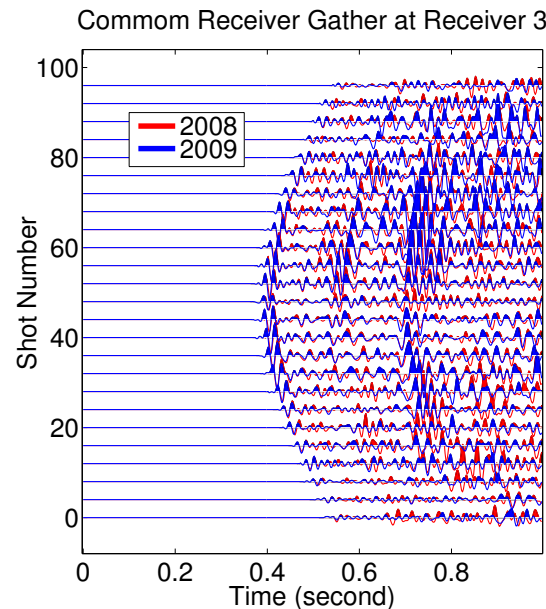


Figure 2: Upgoing waveforms of the baseline walkaway VSP survey in 2008 (in red) and those of the repeat survey in 2009 (in blue) recorded by the third borehole receiver. The data were acquired at an EOR field at SACROC.

and example upgoing waveforms are shown in Figure 1. Additional steps are taken to equalize the different data sets including statics corrections, match filtering and gain equalization. The time-lapse VSP data are balanced against the baseline data using the spectral ratios of upgoing waves reflected from regions above the reservoir. As shown in Figure 2, the first reflection signals from both data sets are of the same amplitude and travelttime.

Double-difference waveform inversion

INITIAL VELOCITY MODEL

A layered velocity model obtained from the zero-offset VSP data is used as the initial model for the waveform inversion of the baseline data. The model and a sonic log are shown in Figure 3. However, the logging profile only reaches to 2134 meters in depth, which is shallower than the depth where the strong reflections (around 0.8 second shown in Figure 2) occur. We use zero-offset traces to conduct a simple velocity analysis and add a few more layers to the model, which generate the later reflections.

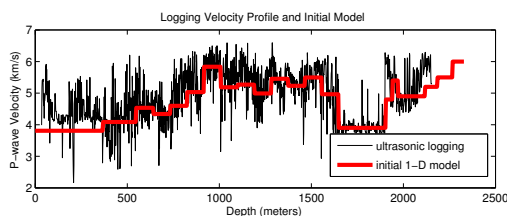


Figure 3: Sonic log profile and the initial 1-D velocity model for waveform inversion.

INVERSION SETUPS AND ASSUMPTIONS

We use the vertical component of the data for this study. The dominant energy in the vertical component of the data is from P-waves. We use the Gardner equation to estimate the density model from the P-wave velocity model (Gardner et al., 1974). The density model is not updated in this study, and we invert for only the P-wave velocity.

We use a 2-D inversion scheme for the walkaway VSP data. The amplitudes of forward modeling waveforms are compensated for the difference between 3-D geometric spreading inherent in the field data and 2-D geometric spreading of the modeling by applying a T-gain (multiply the data by \sqrt{t} where t is time). In addition, the waveforms for 2-D propagation contain a $\frac{\pi}{4}$ phase shift, so we adjust the phase of the data to ensure that there is no phase shift when comparing the synthetics to the data. In addition, arrivals later than those from the strongest reflections, or incoherent signals as shown in Figure 2, are muted as shown in Figure 4. The muted signals are primarily from the region beneath the reservoir.

A time-domain finite-difference scheme with a perfectly matched layer absorbing boundary condition is used for forward modeling. Common-receiver gathers are used for waveform inversions. To reduce the S-wave contamination, only the data from 97 shots and 5 receivers are used.

RESULT

The synthetic waveforms in Figure 4 computed using the initial model contain most of the wave events in the field data, showing two dominant reflections from the top and the bottom of the reservoir. After the baseline inversion, the waveform

fitting is greatly improved, as depicted in Figure 4. The updated baseline model is shown in Figure 5. The updated part has a limited horizontal extent due to the limited illumination coverage of the walkaway VSP surveys.

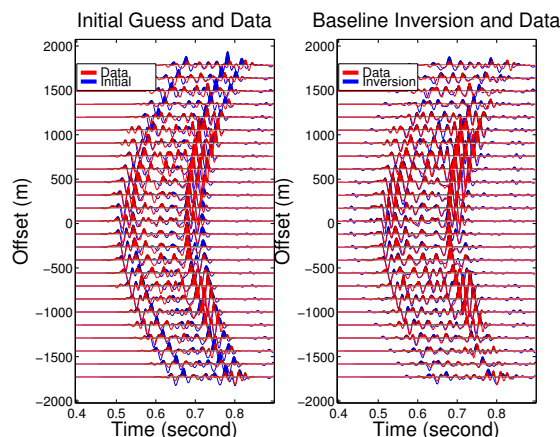


Figure 4: Comparisons of the field VSP data with synthetic waveforms computed using the initial velocity model (left panel) and the updated velocity model obtained from waveform inversion of the baseline VSP data (right panel).

We conduct acoustic double-difference waveform inversion using the time-lapse walkaway VSP data from SACROC, and compare the result with that of the conventional inversion approach with two independent waveform inversions.

Figure 5 shows the waveform inversion result of the baseline, 2008 data. The velocity update to the starting model for the inversion of the 2009 data is displayed in the left panel of Figure 6. It contains similar structures and patterns as those in the right panel of Figure 5. Conventionally, the reservoir change is obtained by subtracting the time-lapse images. The difference between the time-lapse images is shown in the right panel of Figure 6. Some changes are resolved within the reservoir depth (1820 to 2100 meters) by the subtraction, but significant artifacts contaminate the image.

Figure 7 shows the results of our acoustic double-difference waveform inversion of the time-lapse walkaway VSP data from SACROC. The result in the left panel of Figure 7 contains inversions of both reflection and transmission (e.g. tomography) portions of the waveforms. We separate both the forward and backward wavefields into upgoing and downgoing waves again, and calculate the tomographic gradient by cross-correlating the wavefields propagating in the same directions (Mora, 1989). The result, shown in the right panel of Figure 7, gives a much cleaner image of the zones with decreased velocity. Although the image is smeared rather than well-bounded, the volumetric information about the reservoir change is exhibited clearly. The double-difference tomography minimizes the waveform differences caused by phase shifts, related to the velocity decrease.

Double-difference waveform inversion

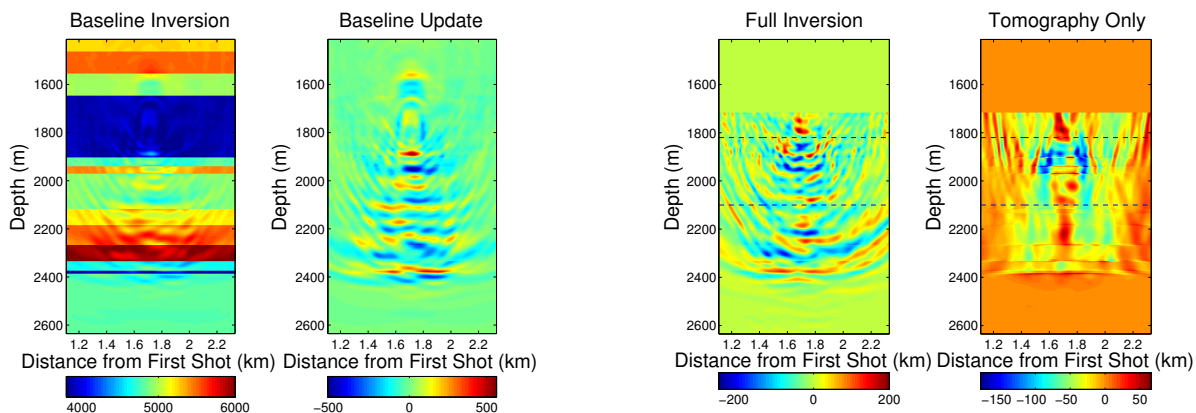


Figure 5: Left: The velocity model obtained from waveform inversion of the baseline walkaway VSP data. Right: The velocity update to the initial model.

Figure 7: The result of acoustic double-difference waveform inversion is shown on the left panel, with the tomography part of the result on the right panel, indicating some regions with decreased velocity within the reservoir.

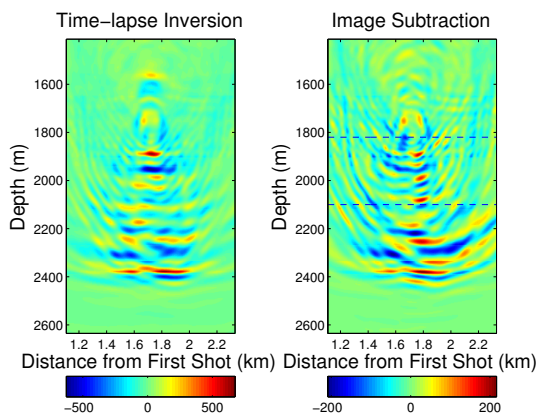


Figure 6: Independent waveform inversions of the time-lapse walkaway VSP data from SACROC. The left panel shows the update of the velocity model for the 2009 data and the right panel shows the image difference between baseline and time-lapse inversions of the 2008 and 2009 data

ACKNOWLEDGMENTS

This work was supported by U.S. DOE/NETL through contract DE-AC52-06NA25396 to Los Alamos National Laboratory, and the MIT Energy Initiative Seed Fund.

CONCLUSIONS

We have applied acoustic double-difference waveform tomography to the time-lapse walkaway VSP data from a SACROC EOR field for monitoring CO₂ injection, and compared the result with that obtained using independent inversions of time-lapse data. Double-difference waveform tomography produces an image showing some reservoir zones with decreased P-wave velocity due to CO₂ injection and migration. These zones cannot be seen in the results of the conventional approach using independent waveform inversions of time-lapse seismic datasets.

EDITED REFERENCES

Note: This reference list is a copy-edited version of the reference list submitted by the author. Reference lists for the 2011 SEG Technical Program Expanded Abstracts have been copy edited so that references provided with the online metadata for each paper will achieve a high degree of linking to cited sources that appear on the Web.

REFERENCES

- Arts, R., O. Eiken, A. Chadwick, P. Zweigel, L. Van der Meer, and B. Zinszner, 2004, Monitoring of CO₂ injected at Sleipner using time-lapse seismic data: *Energy*, **29**, no. 9-10, 1383–1392, [doi:10.1016/j.energy.2004.03.072](https://doi.org/10.1016/j.energy.2004.03.072).
- Bickle, M., A. Chadwick, H. Huppert, M. Hallworth, and S. Lyle, 2007, Modelling carbon dioxide accumulation at Sleipner: Implications for underground carbon storage: *Earth and Planetary Science Letters*, **255**, no. 1-2, 164–176, [doi:10.1016/j.epsl.2006.12.013](https://doi.org/10.1016/j.epsl.2006.12.013).
- Cheng, A., L. Huang, and J. Rutledge, 2010, Time-lapse VSP data processing for monitoring CO₂ injection: *The Leading Edge*, **29**, 196–199, [doi:10.1190/1.3304824](https://doi.org/10.1190/1.3304824).
- Denli, H., and L. Huang, 2009, Double-difference elastic waveform tomography in the time domain: 79th Annual International Meeting, SEG, Expanded Abstracts, 2302–2306, [doi:10.1190/1.3255320](https://doi.org/10.1190/1.3255320).
- Gardner, G., L. Gardner, and A. Gregory, 1974, Formation velocity and density — The diagnostic basics for stratigraphic traps: *Geophysics*, **39**, 770–780, [doi:10.1190/1.1440465](https://doi.org/10.1190/1.1440465).
- Mora, P., 1989, Inversion = migration + tomography: Proceedings of the Shell conference on parallel computing: Springer Verlag, 78–101.
- Onishi, K., T. Ueyama, T. Matsuoka, D. Nobuoka, H. Saito, H. Azuma, and Z. Xue, 2009, Application of crosswell seismic tomography using difference analysis with data normalization to monitor CO₂ flooding in an aquifer: *International Journal of Greenhouse Gas Control*, **3**, no. 3, 311–321, [doi:10.1016/j.ijggc.2008.08.003](https://doi.org/10.1016/j.ijggc.2008.08.003).
- Rodi, W., and R. Mackie, 2001, Nonlinear conjugate gradients algorithm for 2-D magnetotelluric inversion: *Geophysics*, **66**, 174–187, [doi:10.1190/1.1444893](https://doi.org/10.1190/1.1444893).
- Sheen, D., K. Tuncay, C. Baag, and P. Ortoleva, 2006, Time domain Gauss–Newton seismic waveform inversion in elastic media: *Geophysical Journal International*, **167**, no. 3, 1373–1384, [doi:10.1111/j.1365-246X.2006.03162.x](https://doi.org/10.1111/j.1365-246X.2006.03162.x).
- Tarantola, A., 1984, Inversion of seismic reflection data in the acoustic approximation: *Geophysics*, **49**, 1259–1266, [doi:10.1190/1.1441754](https://doi.org/10.1190/1.1441754).
- Watanabe, T., S. Shimizu, E. Asakawa, and T. Matsuoka, 2004, Differential waveform tomography for time-lapse crosswell seismic data with application to gas hydrate production monitoring: 74th Annual International Meeting, SEG, Expanded Abstracts, 2323–2326.